Nucleic Acids Research, 1993, Vol. 21, No. 8 1789–1796

Effect of the non-conserved N-terminus on the DNA binding activity of the yeast TATA binding protein

Ruhul Kuddus and Martin C.Schmidt*
Department of Molecular Genetics and Biochemistry, University of Pittsburgh School of Medicine, Pittsburgh, PA 15261, USA

Received January 25, 1993; Revised and Accepted March 12, 1993

ABSTRACT

We have studied the DNA binding activity of recombinant yeast TATA Binding Protein (TBP) with particular interest in the role played by the non-conserved N-terminal domain. By comparing the DNA binding activity of wild type yeast TBP with a mutant form of TBP that lacks the non-conserved N-terminal domain (TBPΔ57), we have determined that the N-terminus of TBP alters both the shape and the stability of the TBP – DNA complex. Measurements of the DNA bending angle indicate that the N-terminus enhances the bending of the DNA that is induced by TBP binding and greatly destabilizes the TBP – DNA complex during native gel electrophoresis. In solution, the N-terminus has only a slight effect on the equilibrium dissociation constant and the dissociation rate constant. However, the N-terminal domain reduces the association rate constant in a temperature dependent manner and increases the apparent activation energy of the TBP – DNA complex formation by 3 kcal/mole. These data suggest that a conformational change involving the N-terminus of TBP may be one of the isomerization steps in the formation of a stable TBP – DNA complex.

INTRODUCTION

The TATA binding protein (TBP) is a sequence specific DNA binding protein that interacts with TATA box element present in most RNA polymerase II and some RNA polymerase III transcribed gene promoters (1, 2). TBP is one subunit of the multisubunit general factor TFIID required for all RNA polymerase II transcription (3, 4). In addition, TBP is one of the subunits of distinct multisubunit general factors required by RNA polymerase I (5) and RNA polymerase III (6) and thus plays a central role in the initiation of nuclear RNA synthesis by all three polymerase enzymes. For RNA polymerase II transcribed genes that contain TATA elements, TBP is presumably the subunit of the TFIID complex that directs TFIID to the promoter by direct binding the TATA element. TBP complexes may interact with TATA-less promoters through a combination of protein–protein interactions and sequence nonspecific DNA binding. Chemical protection assays indicated that TBP contacts the TATA element in the minor groove (7, 8). Recent structural studies of TBP using on X-ray crystallography indicate that TBP folds into a convex 'saddle' that contacts the DNA via a surface composed of a 10 stranded beta sheet (9).

The genomic and cDNA clones encoding TBP have been isolated from a number of species including fungi, insects, plants, mammals, protozoa and slime mold (10–23). TBP is bipartite with a highly conserved carboxyl terminal core domain of 180 amino acids (~80% sequence identity between all species) and an amino terminus that is variable in length (18–173 residues) and in sequence. *Saccharomyces cerevisiae* TBP is a single polypeptide of 240 residues and an amino terminal domain of 60 residues (22). Biochemical and genetic experiments revealed that the conserved core domain of yeast TBP is necessary and sufficient for sequence specific DNA binding in vitro (24, 25) as well as for basal and activated transcription both in vivo (26–28) and in vitro (29). What then is the biological function, if any, of the N-terminal domain of TBP?

Experiments in which the N-terminal domain is removed have suggested a role for this domain in protein–protein and protein–DNA interactions. Deletion of the N-terminal domain of the human or *Drosophila* TBP results in a loss of responsiveness to the transcriptional activator Sp1 (30, 31), suggesting a role in protein–protein interactions that regulate the transcriptional activity of the TFIID complex. Overexpression of a TBP lacking the N-terminal domain in some yeast strains results in severe growth inhibition and defects in transcriptional activation in vivo (32). Other experiments suggest a role for the N-terminal domain in regulating the DNA binding activity of the C-terminal domain since removal of all or parts of the N-terminus by proteolysis or mutagenesis resulted in a protein with enhanced DNA binding activity (24, 25). Furthermore, full length TBP has the unusual property of binding DNA in a temperature dependent manner and the removal of the N-terminus relaxes this temperature dependence (25). The temperature dependence of DNA binding and changes in the protease sensitivity of TBP upon DNA binding led us to propose TBP undergoes a conformational change upon DNA binding that may be the temperature dependent step of TBP–DNA interactions (25). Alternatively, the recent finding that TBP induces a bend in the DNA upon binding (33) suggests that the temperature dependent step may be a

* To whom correspondence should be addressed

conformational change in the DNA and not the protein. Recent kinetic studies by Hawley and coworkers (34) suggest one or more isomerization steps in the protein and/or the DNA are in the pathway to the formation of a stable TBP−DNA complex.

To address the role played by the N-terminus of TBP in the DNA binding and bending activities of TBP, we have characterized the DNA binding activity of recombinant full length yeast TBP and a mutant form of the protein lacking the N-terminus (TBPΔ57). We find that the N-terminus enhances the TBP-induced DNA bending and that the magnitude of the DNA bend is not temperature dependent. Furthermore, the N-terminus of TBP reduces the stability of the TBP−DNA complex and increases the apparent activation energy barrier for TBP−DNA complex formation.

MATERIALS AND METHODS

DNA preparations

Plasmid pAE4 was constructed by inserting the 90 bp *Hae*III fragment containing the Adenovirus major late promoter (−62 to +28 relative to the initiation site) into the *Sma* I site of pUC18 (35). The adenovirus major late promoter TATA box has the sequence TATAAAA. Plasmid pUCB2 was constructed by inserting the 242 bp *Hind* III−*Eco*RI fragment pBend2 (36) into the *Hind* III and *Eco* RI sites of plasmid pUC18. Complementary oligonucleotides (5′-TCGACTATAAAAG-3′ and 5′-TCGAC-TTTTATAG-3′) containing a consensus TATA box (TATAAAA) with *Sal* I compatible termini were annealed, phosphorylated and cloned into the *Sal* I site of pUCB2 to yield pBTA. The inserts of pBTA and pAE4 were sequenced to confirm the identity of these constructs.

DNA binding probe from pAE4 was prepared by cleavage of the plasmid with *Eco*RI and *Xba*I to release a 120 bp fragment that was labeled with [α-^{32}P]dATP by Klenow enzyme in the presence of unlabeled dCTP, dGTP and dTTP. Circularly permuted probes were generated by digesting pBTA with appropriate restriction endonucleases (Figure 1). All probes with 5′ overhangs were labeled by end filling with [α-^{32}P]dATP or [α-^{32}P]dCTP and Klenow enzyme in the presence of the appropriate unlabeled deoxynucleoside triphosphates. Blunt ended probes were dephosphorylated with alkaline phosphatase and then labeled by phosphorylation with T4 polynucleotide kinase and [γ-^{32}P]ATP. After labeling, the probes were purified from 5% polyacrylamide gel slices using the crush and soak elution protocol (37). The specific activity of different probes were typically $3-6\times10^6$ cpm/pmole.

Purification of yeast TATA binding proteins

The open reading frames for yeast TBP gene (38) and a deletion mutant lacking amino acids 2−57 (TBPΔ57) (M. C. Schmidt, unpublished) have been cloned into *E.coli* T7 expression vector pET3B (39) to generate pKA9 and pKA57. TBP and TBPΔ57 were purified from recombinant bacteria carrying pKA9 or pKA57 essentially as described (22). Both proteins were approximately 30−50% pure as judged by Coomassie blue stained SDS−polyacrylamide gels. The concentration of active protein was calculated using electrophoretic mobility shift assays with 1.0 nM labeled DNA fragment and titrating in 0.060−4.2 pmoles of unlabeled DNA fragment (40).

Electrophoretic mobility shift assays (EMSA)

DNA binding activity of TBP and TBPΔ57 were assayed by EMSA. Radioactivity was quantitated by scintillation counting of dried gel slices containing the free and bound DNA complexes labeled with [^{32}P]. Standard reactions (20 μl) containing 10 nM TBP, 0.5 nM [^{32}P] labeled DNA probe, 4 mM Tris pH 8.0, 5 mM $MgCl_2$, 60 mM KCl, 50 μg/ml poly(dG-dC)-poly(dG-dC), 0.1% Brij 58, 100 μg/ml bovine serum albumin and 4% glycerol, were incubated 60 minutes at room temperature (22°C). 2.5 μg/ml salmon sperm DNA was added in some reactions (noted in the figure legends) to prevent poly(dG-dC)-poly(dG-dC) resistant complex formation. The reactions were then analyzed on 6% polyacrylamide gel (29.2: 0.8, acrylamide: bis) with the electrophoresis buffer containing 25 mM Tris pH 8.3, 190 mM glycine, 5 mM magnesium acetate and 1 mM EDTA. The gel was cast in electrophoresis buffer supplemented with 5 mM magnesium acetate, 0.5 mM DTT and 2.5% glycerol. Electrophoresis was at 10 volts/cm for 3−10 hours. Gels were then transferred to Whatman filter paper, dried under vacuum and exposed to film. Free and bound DNA bands were located on the Whatman filter, excised and radioactivity was quantitated by liquid scintillation counting. Radioactivity scattered between bound and free bands was considered to be free probe. The fraction of DNA bound (f) was defined as follows:

$$f = \frac{moles_{bound}}{moles_{bound} + moles_{free}}$$

Estimation of TBP induced DNA bend angle and bend center

TBP induced bending of DNA was measured by EMSA using DNA fragments containing circularly permutated binding sites (41). Relative mobility (Rf) of TBP−DNA complexes was defined as follows:

$$Rf = \frac{cm_{complex}}{cm_{free}}$$

The length of the different probes varied from 133 bp to 137 bp due to sequence of the pBend polylinker and the difference in labeling procedures (end filling vs. kinasing). To adjust for the slight differences in probe length, the relative mobility's of the TBP−DNA complexes were normalized against highest mobility free probe (42). The average relative mobility from duplicate experiments was plotted as a function of the fractional distance. Fractional distance is defined as the length in base pairs from the center of TATA box element (TATAAAA) to the 5′ end of the noncoding strand of the DNA fragment divided by the total length of the DNA fragment. The data, when plotted as relative mobility versus fractional distance, could be approximated by a least squares fit to the equation $y = ax^2 + bx + c$. The bend point (y = minimum) was determined by setting dy/dx to zero and solving for x. To determine bending angle, we have used the mathematical treatment derived by Ferrari et al (43) where the angle of flexure, θ, is determined from the values for a, b and c are taken from the least squares fit to the quadratic equation using the the following equation: a (or -b) = $2c(1 + \cos\theta)$. With this method, the values for a and -b should be close to identical and offer a means to estimate the error in the measuement of the bending angle. The angle of deviation from linearity, α, is related to θ by the equation $\alpha = 180° - \theta$.

Determination of dissociation rate constants of TBP–DNA complex

The dissociation of TBP–DNA complex in solution and in the gel during electrophoresis was measured by a method similar to that described by Hoopes et al. (34). Both the dissociation reactions follow first order kinetics with a rate equation

$$\frac{-dC}{dt} = kC$$

which upon integration gives

$$\ln C = \ln C_o - kt$$

where C_0 is initial concentration of the TBP–DNA complex, C is concentration of TBP–DNA at time t and k is first order dissociation rate constant. To measure dissociation during electrophoresis, TBP or TBPΔ57 (15 nM) was bound to equilibrium with TATA probe by incubation for 60 minutes at room temperature (22°C) in a volume of 250 μl, 20 μl aliquots were taken and quenched by the addition of a double stranded oligonucleotide containing the sequence of the adenovirus major late promoter TATA box element and immediately loaded onto a 6% EMSA gel. Samples were loaded at several time points during the three hours of electrophoresis. The gel was dried, radioactivity quantitated, and the fraction of the total probe that was present in the bound complex was calculated and plotted as *lnC* versus time. The slope of this line is equal to the negative of the first order rate constant for dissociation during electrophoresis.

To determine the first order rate constant of dissociation in solution, TBP or TBPΔ57 (5 nM) was bound to equilibrium with TATA probe (0.5 nM) by pre-incubating for 60 minutes at room temperature (22°C). At time 0, poly(dA-dT)-poly(dA-dT) was added to final concentration of .05 mg/ml to adsorb unbound TBP and to prevent reassociation of TBP that had dissociated after time t. Aliquots were loaded on a 6% EMSA gel at several time points, and the fraction of the total probe that was bound by TBP was measured for each time point. Because the wild type TBP dissociates during electrophoresis, control reactions in which TBP or TBPΔ57 were bound to equilibrium were loaded in parallel on the same gel. The fraction bound was corrected using the equation

$$F_{cor} = F_{obs}e^{kt}$$

where F_{cor} is the corrected value of the fraction of probe bound, F_{obs} is the observed fraction of probe bound at time *t*, and *k* is the first order dissociation rate constant for the TBP–DNA complex during electrophoresis determined from the control reactions run in parallel (34). The rate constant for dissociation in solution was then determined from the slope of the plot, lnF_{cor} versus time.

Determination of apparent equilibrium dissociation constant (K_{app})

The apparent equilibrium dissociation constant for the TBP–DNA complex was determined by Scatchard plot analysis. A series of standard binding reactions containing a constant amount of TBP protein (10 nM) was incubated with increasing concentrations of the 120 bp DNA fragment containing adenovirus major late promoter TATA box (0.25–20 nM). Bound and free DNA fragments were separated by EMSA and the radioactivity in each fraction was quantitated. The fraction of probe bound was calculated and corrected to compensate dissociation during electrophoresis. For each experiment, dissociation in the gel was determined from reactions run in parallel. The corrected data was plotted as the ratio of bound and free probe versus the concentration of DNA bound. The apparent equilibrium dissociation constant was determined from the Scatchard equation:

$$\frac{[bound]}{[free]} = \frac{-1}{K_{app}}[bound] + \frac{nP}{K_{app}}$$

Where[*bound*] and [*free*] are the concentrations of bound and free DNA fragments, respectively, *P* is concentration of total active protein, n is number of DNA binding sites per protein molecule (assumed to be 1) and K_{app} is the apparent equilibrium dissociation constant. The slope of the Scatchardplot is $-1/Kapp$. In this analysis, the value of *Kapp* is an underestimate of the intrinsic equilibrium constant (Kd) since the nonspecific binding of protein with the poly (dG-dC)-poly (dG-dC) present in each reaction is not taken into account.

Determination of association rate constant (k_{on}) and apparent activation energy (Ea) of binding

A pseudo-first order association rate constant can be determined for second order reactions by making one of the reactants in such excess that its concentration does not appreciably change during the course of the reaction. In this case, the reactions contained 4 nM TBP or TBPΔ57 and 40–60 nM DNA. Binding was initiated by adding protein to prewarmed reactions. Aliquots were removed at increasing times, quenched by the addition of poly(dA-dT)-poly(dA-dT) and immediately loaded onto an EMSA gel. Control reactions in which TBP or TBPΔ57 was bound to TATA probe to equilibrium were run in parallel to control for the dissociation of the TBP–DNA complex during electrophoresis. The fraction of probe bound at each time point was determined and corrected to compensate for dissociation in the gel. The apparent pseudo first order rate constant was determined from the rate law

$$\ln(A_\infty - A) = \ln(A_\infty - A_0) - k't$$

where A_∞, A and A_0 are moles of probe bound at time infinity, at time t and at time 0, respectively, and k′ is the pseudo first order rate constant. k′ can be determined from a plot of $\ln(A_\infty - A)$ versus time (44). Moles of DNA bound at infinity was determined by plotting moles bound versus time and fitting the curve to the non-linear least square equation

$$A = A_\infty(1 - e^{-kt})$$

where k is a constant.

The apparent activation energy of DNA binding (*Ea*) was determined from the pseudo first order association rate constants determined at two different temperatures from Arrhenius equation:

$$\ln\left(\frac{k'2}{k'1}\right) = \frac{-Ea}{R\left(\frac{1}{T_2} - \frac{1}{T_1}\right)}$$

where k'_1 and k'_2 are pseudo first order association rate at temperature T_1 and T_2 (in degrees Kelvin) and R is the universal gas constant.

RESULTS

Effect of the non-conserved N-terminus of TBP on DNA bending

To measure the DNA bending induced by TBP, EMSA assays were performed with a series of labeled DNA fragments with circularly permutated TBP binding sites. The set of DNA fragments used in this experiment is diagrammed in Figure 1A. The effect of the non-conserved N-terminus of TBP on DNA bending was determined by comparing the DNA bend induced by wild type TBP with that induced by a deleted form of TBP from which the entire non-conserved N-terminus was deleted (TBPΔ57). TBP and TBPΔ57 were bound to the circularly permuted probes and the DNA–protein complexes were resolved in non-denaturing polyacrylamide gels. Both the TBP–DNA complex and the TBPΔ57–DNA complex migrated with reduced mobility when the TATA box was present at the center of the probe relative to the mobility of the complex formed when the TATA box was present near the end of the probe. The difference in mobility of the DNA–protein complexes due to the position of the binding site indicates DNA bending (45). A plot of the relative mobility's of TBP–DNA complexes as a function of fractional distance from the center of the TATA box to the 5′ end of the noncoding strand yielded a U-shaped curve (Figure 1B). The center of bending, defined as the minimum of the U-shaped curve, fell within the TATA box sequence for both TBP and TBPΔ57. Applying the mathematical relationship developed by Ferrari et al. (43), we find that the bending angles (α) induced by TBP and TBPΔ57 at room temperature are 75° ± 1.5° and 62° ± 1.5°, respectively. Therefore, the non-

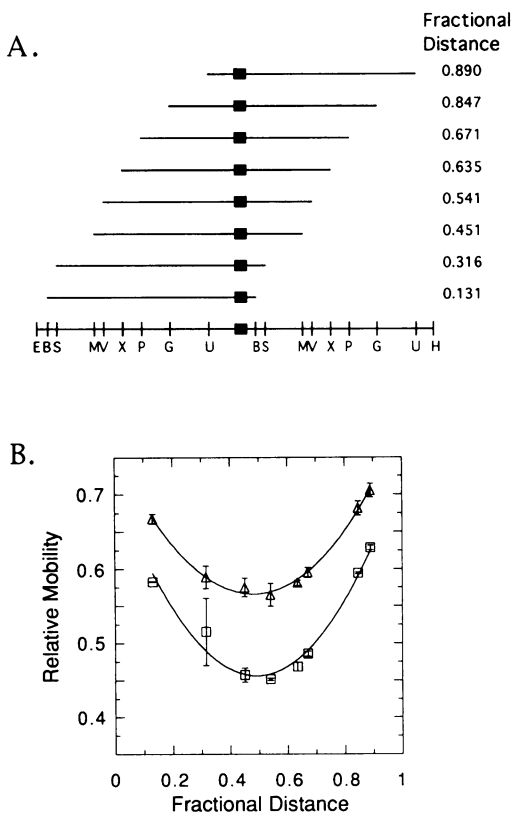

Figure 1. DNA bending: **A.** Circularly permuted binding site probes. The set of eight circularly permuted DNA fragments generated by cleavage of plasmid pBTA with different restriction endonucleases are drawn to scale. The fractional distance of the center of the binding site (TATAAA, shown as a solid rectangle) relative to the 5′ end of the noncoding strand is shown to the right of each probe. The abbreviations used for the restriction endonucleases are E, *Eco* RI; B, *Bam* HI; S, *Ssp* I; M, *Sma* I; V, *Eco* RV; X, *Xho* I; P, *Spe* I; G, *Bgl* II; U, *Mlu* I; H, *Hind* III. **B.** Relative mobilities of TBP–DNA complexes. TBP–DNA and TBPΔ57–DNA complexes were separated from free DNA by EMSA. The mobility of the complex relative to the mobility of the free DNA fragment is plotted against fractional distance of the center of the TATA element to the 5′ end of the noncoding strand. The data plotted are the average of two experiments. The data for TBP (□) and TBPΔ57 (△) were fitted to the equations $y = 1.06 X^2 - 1.04X + 0.71$ ($R = 0.984$) and $y = 0.83 X^2 - 0.81X + 0.76$ ($R = 0.997$), respectively. The values for the first order and second order terms from both experiments were in good agreement for both TBP and TBP-d57 and yield bending angles (α) of 75° ±1.5° and 62° ±1.5°, respectively.

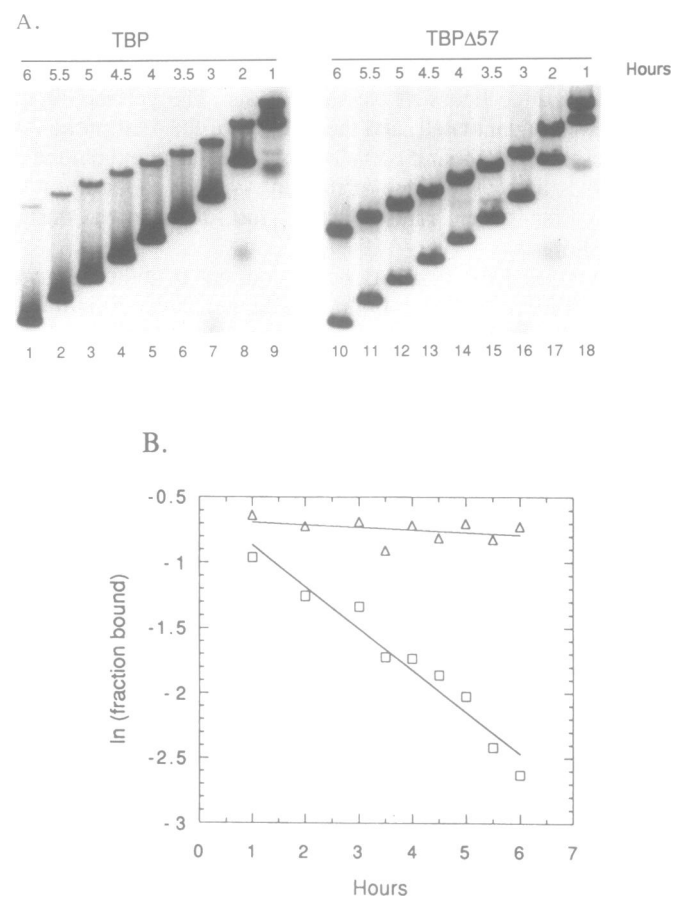

Figure 2. Dissociation of the TBP–DNA complex during electrophoresis. **A.** TBP (lanes 1–9) or TBPΔ57 (lanes 10–18) were bound to equilibrium to a 120 bp probe containing a consensus TATA box element. Aliquots were removed at different times and loaded onto a 6% polyacrylamide gel. Each sample was subjected to electrophoresis at 10 volts/cm for the time indicated above each lane. The gels were then dried and exposed to X-ray film. **B.** Dissociation Rate. The fraction of the DNA probe that was bound by TBP or TBPΔ57 was determined by liquid scintillation counting of excised gel slices. The natural log of the fraction bound (□ for TBP; Δ for TBPΔ57) is plotted versus time. The first order dissociation rate constants, the negative of the slope for each line, were deteremined to be 8.9×10^{-5} sec^{-1} and 5.4×10^{-6} sec^{-1} for TBP and TBPΔ57, respectively.

conserved N-terminus of TBP enhances the DNA bending angle induced by the binding of TBP.

TBP has the unusual property of binding DNA in a temperature dependent fashion. In DNase I footprinting assays, TBP–DNA complexes are difficult to detect at 0°C (46). Removal of the non-conserved N-terminus, however, ameliorates binding at 0°C (25). It was proposed that the requirement for thermal energy reflected a conformational change in TBP. Alternatively, the temperature dependence of binding could reflect an energy requirement needed to bend the DNA helix. To distinguish these possibilities, we tested the ability of TBP to bend DNA at 0°C.

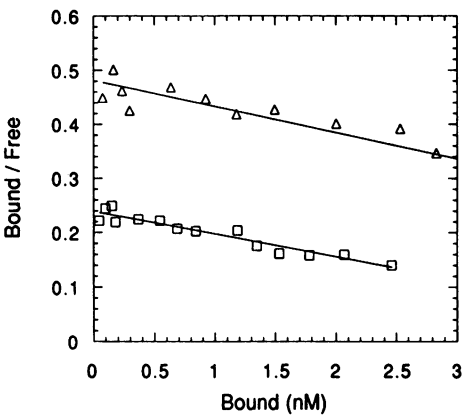

Figure 3. Apparent equilibrium dissociation constant. The affinity of TBP and TBPΔ57 for the TATA box element was determined by Scatchard plot analysis. Reactions containing an invariant concentration of TBP or TBPΔ57 (10 nM) were incubated with increasing concentration of DNA (0.25–20 nM) for sufficient time to reach equilibrium. Bound and free DNA fragments were resolved by EMSA quantitated by liquid scintillation counting of excised gel slices. The ratio of the moles of bound DNA to the moles of free DNA is plotted against the concentration (nM) of bound DNA for TBP (□) and TBPΔ57 (△). The apparent equilibrium dissociation constants (Kapp), calculated as the negative reciprocal of the slopes, were determined to be 24 nM and 21 nM for TBP and TBPΔ57, respectively.

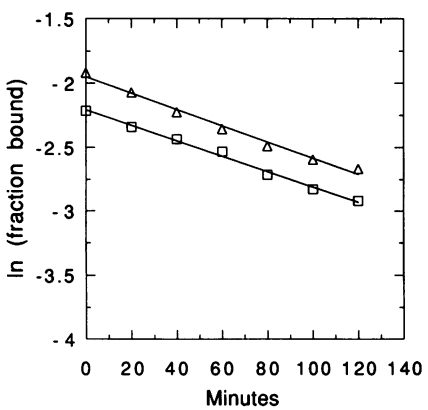

Figure 4. Rate of complex dissociation in solution. The dissociation of the TBP–DNA complexes was measured by challenging reactions at equilibrium with excess unlabeled poly(dA-dT)-poly(dA-dT) at time 0. Aliquots were removed at increasing times and the fraction of DNA bound was determined by EMSA. The natural log of the fraction of the DNA bound for TBP (□) and TBPΔ57 (△) is plotted against time. The first order dissociation rate constants, calculated as the negative of the slopes, were determined to be 1.0×10^{-4} sec^{-1} and 1.1×10^{-4} sec^{-1} for TBP and TBPΔ57, respectively.

TBP or TBPΔ57 was incubated with the set of DNA fragments with circularly permuted binding sites at 0°C and the complexes were resolved by EMSA at 4°C. We observed that both proteins were able to bind and to bend DNA at 0°C; TBP bound very poorly, but detectably at 0°C (data not shown). Analysis of the bend angle and bend center revealed that there was no significant differences between the values at 0°C and those at 22°C (data not shown). Thus, once the TBP–DNA complex forms, its structure, as measured by the angle of DNA bending, is independent of temperature.

The circular permutation assay used here cannot distinguish between DNA bending and an increased flexibility in the DNA at the point of protein binding (47). However, DNA flexibility is predicted to increase in response to increased temperature (48), a prediction that is not consistent with our data. The calculated bending angle for the TBP–DNA complex was 75° at both 22°C and at 4°C. Thus the altered mobility of the TBP–DNA complex in the circular permutation assay is not due to induced DNA flexibility. The TBP–DNA complex exists in a defined structure in which the DNA is bent, independent of temperature.

Effect of the N-terminus of TBP on dissociation of the TBP–DNA complex during electrophoresis

Earlier studies indicated that the N-terminus of TBP interfered with DNA binding (24, 25) although the mechanism of this inhibition was not known. Recent findings by Hawley and colleagues indicated that the TBP–DNA complex was particularly unstable during native gel electrophoresis (34). One indication of the dissociation of the TBP–DNA complex during electrophoresis is the appearance of a heterogeneous region (smear) of radioactivity with a mobility intermediate between that of the DNA–protein complex and that of the free probe. Based on this criterion, we noticed that DNA–protein complexes formed with TBPΔ57 showed much less dissociation during electrophoresis than TBP–DNA complexes (Figure 2A). We determined the first order dissociation rate constants (k_{off}) of both the TBP–DNA complex and the TBPΔ57–DNA complex during electrophoresis under identical assay conditions to be 8.9×10^{-5} sec^{-1} and 5.4×10^{-6} sec^{-1}, respectively (Figure 2B). The TBP–DNA complex dissociates during electrophoresis with a half time of 2.2 hour, which is significant considering the electrophoresis time for these gels is on the order of 2–4 hours. In contrast, the TBPΔ57–DNA complex is much more stable during electrophoresis with a half time of 35 hours.

Effect of the N-terminus of TBP on the apparent equilibrium dissociation constant

Since the N-terminus of TBP was found to have a large effect on the stability of the TBP–DNA complex during electrophoresis, it was of interest to determine the effect of the N-terminus on the DNA binding activity of TBP in solution. The overall affinity of TBP and TBPΔ57 for the TATA box element was determined by measuring the apparent equilibrium dissociation constant (Kapp) using Scatchard plot analysis. TBP–DNA complexes were formed in the presence of increasing concentrations of DNA fragment and a constant concentration of TBP (Figure 3). Free DNA and DNA bound by TBP were separated by EMSA and the values corrected for dissociation during electrophoresis. The Kapp's for TBP and TBPΔ57 were 2.4×10^{-8} M and 2.1×10^{-8} M, respectively. These data indicate that removal of the N-terminus from TBP only slightly

increases the protein's affinity for its DNA ligand in solution. Using the y-intercept, the number of DNA binding sites per protein were calculated to be 1.0 for TBP and 1.1 for TBPΔ57. The difference in the y-intercept values for TBP and TBPΔ57 is due to the difference in the concentration of active protein in the reactions, 6.5 nM for TBP and 10 nM for TBPΔ57 and not due to a difference in the number of DNA binidng sites per protein. The small difference in equilibrium dissociation constants contrasts with the finding that the dissociation of TBP–DNA complexes during electrophoresis is enhanced 16 fold by the N-terminus. Since the equilibrium constant is the ratio of the kinetic constants for dissociation and association, it was possible that the N-terminus affected both kinetic rate constants in a way that canceled their effect's on the equilibrium constant. To test this possibility, both the first order dissociation rate constants and the pseudo-first order dissociation rate constants for TBP and TBPΔ57 were determined.

Effect of the N-terminus of TBP on the dissociation rate of the TBP–DNA complex in solution

The dissociation of TBP–DNA complexes in solution was measured by challenging preformed complexes at equilibrium with an excess of cold competitor DNA. Any TBP that dissociates from the labeled probe during this incubation is prevented from rebinding the probe by the excess cold competitor. By plotting the natural log of the fraction of probe DNA bound versus time, the first order dissociation rate constant was calculated (Figure 4). The dissociation rate constants for the TBP–DNA complex and the TBPΔ57-DNA complex in solution were 1.0×10^{-4} sec^{-1} and 1.1×10^{-4} sec^{-1}, respectively. These values differ by ~10% and probably do not reflect a significant difference in dissociation rates between these two proteins. The finding that the Kapp's and koff rates for TBP and TBPΔ57 are not significantly different predicts that the association rate constants at room temperature for these proteins will also be very similar.

Effect of the N-terminus on the association rate constant

The binding of TBP to the TATA box element is a second order reaction, dependent on the concentration of both TBP and the DNA ligand. Characterization of the kinetics of TBP–DNA association suggests that the reaction is relatively slow and may involve one or more isomerization steps (34). In order to test the effect of the N-terminus of TBP on the association reaction, we measured the pseudo-first order association rate constants for TBP and TBPΔ57. By keeping the concentration of the DNA probe in excess (60 nM DNA and 4 nM TBP), the concentration of the free DNA probe did not change appreciably during the course of the binding reaction.The pseudo-first order association rate constants for TBP and TBPΔ57 at 22°C and 60 nM DNA were calculated to be 1.5×10^{-3} sec-1 and 1.8×10^{-3} sec-1, respectively (Figure 5A). This small increase in association rate constant due to the removal of the N-terminus is enough to account for the increase in affinity of TBPΔ57 for DNA that is reflected by the decrease in the apparent equilibrium dissociation constant.

Effect of the N-terminus on the apparent activation energy of DNA binding

Earlier studies of TBP's DNA binding activity indicated that its ability to form a stable complex with DNA was temperature dependent (25). This observation leads to the prediction that the association rate for TBP and DNA would be slower at lower temperatures. If true, the difference in association rate constants at different temperatures allows the calculation of the apparent activation energy (Ea) of DNA binding using the Arrhenius equation. The pseudo-first order association rate constants at 0°C were determined to be 5.4×10^{-4} sec^{-1} and 8.6×10^{-4} sec^{-1} for TBP and TBPΔ57, respectively (Figure 5B). Using the Arrhenius equation, the apparent activation energy for DNA binding by TBP and TBPΔ57 is calculated to be 9.4 kcal mol^{-1} and 6.6 kcal mol^{-1}, respectively.

DISCUSSION

Our results indicate that the N-terminal domain affects the structure and the stability of the TBP–DNA complex. Structurally, the N-terminus increases the DNA bending angle of the TBP–DNA complex from 62° in the absence of the N-terminus (TBPΔ57) to 75° in the presence of the N-terminus (TBP). The major effect that the N-terminus has on the stability of the TBP–DNA complex is detected during native gel electrophoresis where the N-terminus increases the dissociation rate of the TBP–DNA complex by a factor of 16. The large difference in dissociation rate during electrophoresis can account for the differences in DNA binding activity detected by electrophoretic mobility shift assays with TBP and derivatives lacking parts (24) or all of the N-terminus (25).

In solution, the N-terminus of TBP has relatively little effect on the DNA binding activity. At room temperature, the apparent equilibrium dissociation constants, the pseudo-first order association rate constants and the dissociation rate constants for TBP and TBPΔ57 all differed by 1.2 fold or less. The largest effect of the N-terminus on DNA binding in solution was evident in the effect of temperature on the pseudo-first order association rate constant. From these data we calculate that the apparent activation energy for complex formation is relatively high and increased further by the presence of the N-terminus. Thus, the N-terminus of TBP exacts an energy cost for DNA binding. Some portion of the increased energy may be due to the increase in DNA bending that occurs when the N-terminus is present. Our data are consistent with the hypothesis that a conformational change involving the N-terminus of TBP is one of the isomerization steps in the formation of a stable TBP–DNA complex. We hypothesize that when TBP is free in solution, the N-terminus is present in a conformation that interferes with the formation of a stable TBP–DNA complex. An isomerization of the complex is required to change the conformation of the DNA and/or the N-terminus of the protein to form a stable TBP–DNA complex. A conformational change in the protein may occur either in solution and prior to DNA binding or subsequent to the formation of an initial, less stable, intermediate complex on the DNA.

The existence of an intial TBP–DNA complex that subsequently isomerizes to form a more stable TBP–DNA complex is supported by the detailed, kinetic studies of Hawley and coworkers (34). In general, the results presented here are in close agreement with that earlier study. The value we calculate for the first order dissociation rate constant of the TBP–DNA complex is similar to the value calculated by Hawley and coworkers (1.0×10^{4} sec^{-1} vs. 1.1×10^{4} sec^{-1}). However, our value for second order association rate constant, calculated by dividing the pseudo-first order rate constant by the concentration of DNA ligand, is lower by a factor of ten than that determined by Hawley and coworkers (2.5×10^{4} $M^{-1}sec^{-1}$ vs. 3.4×10^{5}

$M^{-1}sec^{-1}$). The reason for this discrepancy is likely due to the fact that the association rate for the formation of the TBP–DNA complex is extremely dependent on the concentration of TBP (34). Low concentrations of TBP were the likely reason that earlier studies (25, 46) underestimated the rate of TBP–DNA complex formation. In this study the association reaction was made pseudo-first order by using excess ligand and a relatively low concentration of TBP, which may explain why our values for association rate are lower than those determined using excess TBP.

Of the many methods to assay DNA binding by a protein, the electrophoretic mobility shift assay (EMSA) has become the most widely used due to its ease, sensitivity and utility in assaying specific interactions in unfractionated cell extracts (49). However, the TBP–DNA complex is somewhat unusual by not being easily detected by EMSA using standard electrophoresis buffer conditions. To detect the TBP–DNA complex by EMSA, the complex needs to be stabilized by the addition of magnesium and glycerol to the gel and magnesium to the electrophoresis buffer. Alternatively, the TBP–DNA complex can be stabilized by the presence of additional proteins (TFIIA, TFIIB or Dr1) in the complex (50, 51). The work reported here shows that the instability of the TBP–DNA complex is due to the N-terminus. Removal of the N-terminus greatly stabilizes the TBP–DNA complex during electrophoresis and also makes the complex detectable in a greater number of buffer conditions in the absence of additional proteins (data not shown).

Many DNA–protein complexes dissociate much more slowly during electrophoresis than in solution. This finding may be due to the low ionic strength of the gel system, the increased local concentration of the reactants due to molecular exclusion from the gel matrix or due to the inhibition of diffusion of dissociated molecules by the gel matrix, a phenomenon known as 'caging' (52). Our studies indicate that the N-terminus of TBP blocks the ability of the gel matrix to stabilize the protein–DNA complex. The dissociation rate for the TBP–DNA complex in the gel is almost the same as the rate in solution (0.89 vs 1.0×10^{-4} sec^{-1}). In contrast, removal of the N-terminus results in a stabilization of the TBPΔ57–DNA complex in the gel matrix such that the dissociation rate of the TBPΔ57–DNA complex in the gel is 20 fold slower than the rate in solution (0.054 vs 1.1×10^{-4} sec^{-1}). How does the N-terminus of TBP block the stabilization of the TBP–DNA complex during electrophoresis? One simple explanation would be a charge difference between TBP and TBPΔ57 since a net positive charge on a protein in a native gel would cause the dissociated protein to migrate in the opposite direction from the free DNA and thus hinder reassociation. This is a not the explanation in this case since TBPΔ57 has a slightly greater net positive charge than TBP (+11 vs +7.2 at pH 8) yet it is the TBPΔ57–DNA complex that dissociates 20 times more slowly in the gel than in solution. We favor the hypothesis that it is the rebinding of dissociated TBP that is differentially affected by the N-terminus. This would be consistent with the observation that the apparent activation energy of binding is increased by 3 kcal/mol by the presence of the N-terminus.

What is the biological role of the N-terminal domain of TBP? One possible model that is consistent with the current data is that the function of the N-terminus is to block the formation of protein–protein complexes between TBP and other transcription factors until TBP is correctly positioned on the DNA. The same isomerization step that moves the N-terminus out of the way of the DNA binding domain could expose an interaction surface of TBP. This would ensure that only the TBP molecules that are bound to DNA in productive complexes are able to compete for binding to additional factors. Consistent with this model is the observation that overexpression of TBPΔ57 in vivo causes a severe inhibition of growth in some yeast strains (32). According to this model, high levels of TBPΔ57 are deleterious to yeast because they have a constitutively exposed interaction surface that is titrating an important transcription factor into a non-productive complex. This model also leads to the prediction that the protein that binds the surface exposed by the removal or isomerization of the N-terminus, will have a higher affinity for the TBP–DNA complex or for TBPΔ57 than it does for TBP in solution.

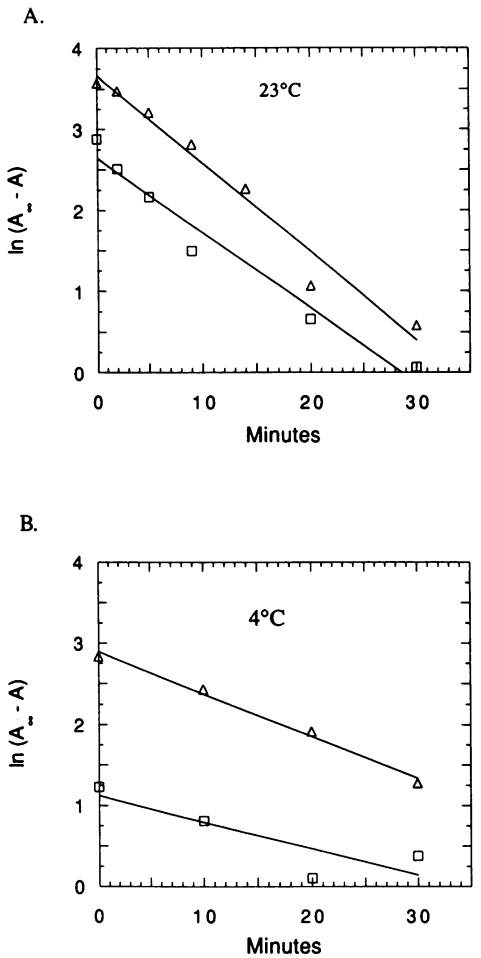

Figure 5. Rate of complex formation. The pseudo-first order association rate constants for the formation of TBP–DNA and TBPΔ57–DNA complexes were determined in reactions containing 4 nM protein and an excess of the DNA ligand (60 nM) at 23°C **(A)** or at 4°C **(B)**. Aliquots were removed after increasing times following the addition of the protein to reactions. Bound and free DNA was separated by EMSA at 23°C or 4°C, and quantitated by liquid scintillation counting of dried gel slices. The data (□ for TBP and △ for TBP-Δ57) are plotted as the natural log of the fraction bound at infinite time (determined empirically) minus the fraction bound at time t versus time. The pseudo-first order association rate constants, calculated as the negative of the slopes, were determined to 1.5×10^{-3} sec^{-1} and 1.8×10^{-3} sec^{-1} for TBP and TBPΔ57, respectively at 23°C and 5.4×10^{-4} sec^{-1} and 8.6×10^{-4} sec^{-1}, for TBP and TBPΔ57, respectively at 4°C.

ACKNOWLEDGMENTS

We are grateful to Karen Arndt for providing pKA9 and to Tommy Tillman, Vicki Nebes and Will McClure for critical reading of this manuscript. This work was supported by a grant from the National Institutes of Health (GM 46443), and an American Cancer Society Junior Faculty Research Award to M.C.S.

REFERENCES

1. Davison, B. L., J. M. Egly, E. R. Mulvihill and P. Chambon (1983) Nature, **301,** 680–686.
2. Simmen, K. A., J. Bernues, H. D. Parry, H. G. Stunnenberg, A. Berkenstam, B. Cavallini, J. M. Egly and I. W. Mattaj (1991) EMBO J., **7,** 1853–1862.
3. Dynlacht, B. D., T. Hoey and R. Tjian (1991) Cell, **66,** 563–576.
4. Pugh, F. B. and R. Tjian (1992) J. Biol. Chem., **267,** 679–682.
5. Comai, L., N. Tanese and R. Tjian (1992) Cell, **68,** 965–976.
6. White, R. J., S. P. Jackson and P. W. J. Rigby (1992) Proc. Natl. Acad. Sci. U.S.A., **89,** 1949–1953.
7. Starr, D. B. and D. K. Hawley (1991) Cell, **67,** 1231–1240.
8. Lee, D. K., M. Horikoshi and R. G. Roeder (1991) Cell, **67,** 1241–1250.
9. Nikolov, D. B., S. Hu, J. Lin, A. Gasch, A. Hoffmann, M. Horikoshi, N. Chua, R. G. Roeder and S. K. Burley (1992) Nature, **360,** 40–46.
10. Cavallini, B., I. Faus, H. Matthes, J. M. Chipoulet, B. Winsor, J. M. Egly and P. Chambon (1989) Proc. Natl. Acad. Sci. U.S.A., **86,** 9803–9807.
11. Eisenmann, D. M., C. Dollard and F. Winston (1989) Cell, **58,** 1183–1191.
12. Fikes, J. D., D. M. Becker, F. Winston and L. Guarente (1990) Nature, **346,** 291–294.
13. Gasch, A., A. Hoffmann, M. Horikoshi, R. G. Roeder and N. H. Chua (1990) Nature, **346,** 390–394.
14. Hahn, S., S. Buratowski, P. A. Sharp and L. Guarente (1989) **58,** 1173–1181.
15. Haass, M. M. and G. Feix (1992) FEBS Lett., **301,** 294–298.
16. Hoey, T., B. D. Dynlacht, M. G. Peterson, B. F. Pugh and R. Tjian (1990) Cell, **61,** 1179–1186.
17. Hoffmann, A., M. Horikoshi, C. K. Wang, S. Schroeder, P. A. Weil and R. G. Roeder (1990) Genes Dev., **4,** 1141–1148.
18. Hoffmann, A., E. Sinn, Y. T., J. Wang, A. Roy, M. Horikoshi and R. G. Roeder (1990) Nature, **346,** 387–390.
19. Horikoshi, M., K. C. Wang, H. Fujii, J. A. Cromlish, P. A. Weil and R. G. Roeder (1989) Nature, **341,** 299–303.
20. Kao, C. C., P. M. Lieberman, M. C. Schmidt, Q. Zhou, R. Pei and A. J. Berk (1990) Science, **248,** 1646–1650.
21. Peterson, M. G., J. Inostroza, M. E. Maxon, O. Flores, A. Admon, D. Reinberg and R. Tjian (1991) Nature, **354,** 369–373.
22. Schmidt, M. C., C. C. Kao, R. Pei and A. J. Berk (1989) Proc. Natl. Acad. Sci. U.S.A., **86,** 7785–7789.
23. Wong, J. M., F. Liu and E. Bateman (1992) Gene, **117,** 91–97.
24. Horikoshi, M., T. Yamamoto, Y. Ohkuma, P. A. Weil and R. G. Roeder (1990) Cell, **61,** 1171–1178.
25. Lieberman, P. M., M. C. Schmidt, C. C. Kao and A. J. Berk (1990) Mol. Cell. Biol., **11,** 63–74.
26. Cormack, B. P., M. Strubin, A. S. Ponticelli and K. Struhl (1991) Cell, **65,** 341–348.
27. Gill, G. and R. Tjian (1991) Cell, **65,** 333–340.
28. Reddy, P. and S. Hahn (1991) Cell, **65,** 349–357.
29. Kelleher, R. J., P. M. Flanagan, D. I. Chasman, A. S. Ponticelli, K. Struhl and R. D. Kornberg (1992) Genes Dev., **6,** 296–303.
30. Peterson, M. G., N. Tanese, F. Pugh and R. Tjian (1990) Science, **248,** 1625–1630.
31. Pugh, B. F. and R. Tjain (1991) Genes Dev., **5,** 1935–1945.
32. Zhou, Q., M. C. Schmidt, P. M. Lieberman and A. J. Berk (1991) EMBO J., **10,** 1843–1852.
33. Horikoshi, M., C. Bertuciolli, R. Takada, J. Wang, T. Yamamoto and R. G. Roeder (1992) Proc. Nat. Acad. Sci. USA, **89,** 1060–1064.
34. Hoopes, B. C., J. F. LeBlanc and D. K. Hawley (1992) J. Biol. Chem., **267,** 11539–11547.
35. Yanish-Perron, C., J. Vieira and J. Messing (1985) Gene, **33,** 103–119.
36. Kim, J., C. Wu and S. Adhya (1989) Gene., **85,** 15–23.
37. Sambrook, J., E. F. Fritsch and T. Maniatis. Molecular Cloning. 1989.
38. Arndt, K. M., S. L. Ricupero, D. M. Eisenmann and F. Winston (1992) Mol. Cell. Biol., **12,** 2372–2382.
39. Studier, F. W. and B. A. Moffatt (1986) J. Mol. Biol., **189,** 113–130.
40. Hahn, S., S. Buratowski, P. A. Sharp and L. Guarente (1989) Proc. Natl. Acad. Sci. U.S.A., **86,** 5718–5722.
41. Thompson, J. F. and A. Landy (1988) Nucl. Acids. Res., **16,** 9687–9705.
42. Karppola, T. K. and T. Curran (1991) Cell, **66,** 317–326.
43. Ferrari, S., V. R. Harley, A. Pontiggia, P. Goodfellow, R. Lovell-Badge and M. E. Bianchi (1992) EMBO J., **11,** 4497–4506.
44. Hinkle, D. C. and M. J. Chamberlin (1972) J. Mol. Biol., **70,** 157–185.
45. Wu, H. M. and D. M. Crothers (1984) Nature, **308,** 509–513.
46. Schmidt, M. C., Q. Zhou and A. J. Berk (1989) Mol. Cell. Biol., **9,** 3299–3307.
47. Zinkel, S. S. and D. M. Crothers (1987) Nature, **328,** 178–181.
48. Schreck, R., H. Zorbas, E. Winnacker and P. A. Beauerle (1990) Nucl. Acids. Res., **22,** 6497–6502.
49. Lane, D., P. Prentki and M. Chandler (1992) Microbiol. Rev., **56,** 509–528.
50. Inostroza, J. A., F. H. Mermelstein, I. Ha, W. S. Lane and D. Reinberg (1992) Cell, **70,** 477–489.
51. Buratowski, S., S. Hahn, L. Guarente and P. A. Sharp (1989) Cell, **56,** 549–561.
52. Fried, M. and D. M. Crothers (1981) Nucl. Acids. Res., **9,** 6505–6525.